Photoacoustic and luminescence spectroscopy of benzil crystals

B. Bonno, J. L. Laporte, and Y. Rousset
Laboratoire d'Optique Moléculaire, Université de Reims, Boîte Postale 347, 51062 Reims CEDEX, France
(Received 9 October 1990; revised manuscript received 27 December 1990)

In the present work, both photoacoustic and luminescence techniques were employed to study molecular crystals. This paper presents an extension of the standard Rosencwaig-Gersho photoacoustic model to molecular crystals, which includes finite-deexcitation-time effects and excited-state populations. In the temperature range 100–300 K, the phosphorescence quantum yield and thermal diffusivity of benzil crystals were determined.

INTRODUCTION

Photoacoustic (PA) spectroscopy has received a considerable amount of attention in recent years owing to its potential advantages in the study of the optical properties of solids.[1]

Recently the PA technique has been applied to the study of molecular crystals,[2,3] and to the determination of the luminescence quantum yields of various materials.[4,5]

Also, the PA technique allows one to determine the thermal properties of solids. Among the several physical parameters to be monitored, the thermal diffusivity α is a particularly important parameter. The importance of α as the physical quantity to be controlled is due to the fact that, like the optical absorption coefficient, it is unique for each material. Several papers have been published on the measurement of the thermal diffusivity for a wide range of materials.[6–9]

In the present work, we investigate polycrystalline samples of benzil ($C_6H_5-CO-CO-C_6H_5$). The luminescence signal and the PA signal for the front surface excitation and the rear surface excitation were analyzed over a large range of temperatures. From these results, we deduced the phosphorescence quantum yield and the thermal diffusivity of benzil crystal versus temperature.

EXPERIMENTAL METHODS AND RESULTS

Polycrystalline samples of benzil from the Aldrich laboratories were purified using zone refining. Crystals were placed inside an optical cryostat, and the temperature was monitored by means of a platinum resistance in contact with the crystal holder.

The photoacoustic cell is a hollow cylinder with a 4 mm diameter and a 3 mm depth sealed by two silica circular windows. The sample is a film of thickness l_s lying on the surface of the sealing discs. These films are obtained by crystallization of polycrystalline benzil on silica and are then polished.

The light beam was modulated by a mechanical chopper. The sample was excited by a 366-nm light beam selected by means of a monochromator from a 200-W mercury lamp (Phillips CS 200 W2).

The PA signal was detected by a 0.5-in condenser microphone (Bruel and Kjaer 4133) with a sensitivity of 12.5 mV Pa^{-1}. The microphone was placed at room temperature and connected to the PA cell by a narrow tube, 0.5 mm in diameter and 9 cm in length, in order to protect it from the low temperature.

The signal amplitude was measured with a lock-in amplifier (P.A.R. 5206). Because the sample chamber was air filled, we could not measure temperatures below 100 K.

From 20 to 100 Hz, and for temperatures between 100 and 300 K, the PA signal emitted by a black carbon sample varies linearly as a function of f^{-1}. We have not observed any changes in the resonance characteristics of the PA cell.

Sample luminescence was obtained from another optical cryostat. The cell used in this case is simply a sample holder. Sample excitation and the temperature measure remained unchanged. Luminescence signals were detected photoelectrically using a M25 Huet monochromator with a resolution of 30 cm^{-1} and a R928 Hamamatsu photomultiplier.

Lifetime values were deduced from the data delivered by a Becquerel-type phosphoroscope; the accumulation of the data was monitored by means of a microprocessor.

At 77 K the benzil phosphorescence spectrum shows a very intense nonstructured band whose maximum intensity is at 526 nm (19 010 cm^{-1}) and whose half width is about 1000 cm^{-1}. In the red region of the spectrum we observed a second peak at 575 nm (17 390 cm^{-1}), less intense than the first, and a shoulder at 635 nm (15 750 cm^{-1}). This fact corresponds to the characteristic valence vibrational frequency of the carbonyl group. No frequency shift was observed on increasing the temperature from 77 to 300 K. There was only a broadening of the bands. These results are in agreement with those obtained by previous workers.[10,11]

The phosphorescence intensity I_p of the benzil 526-nm band as a function of the temperature from 77 to 300 K is shown in Fig. 1. In Fig. 2, we report the phosphorescence lifetimes obtained for variations of the sample temperature between 77 and 250 K. Above 250 K, the phosphorescence intensity is too weak for the phosphorescence lifetimes to be measured. We have studied the PA signal amplitude as a function of the beam frequency

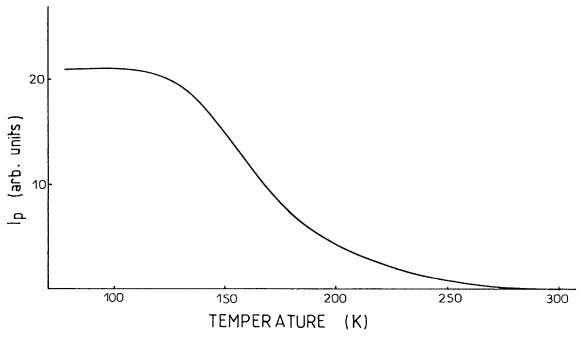

FIG. 1. Variation of phosphorescence intensity I_p with temperature for benzil polycrystalline samples.

modulation for front and rear excitation. In the first case we have used a sample 200-μm thick, and in the second one a sample 100-μm thick. Experimental results for different temperatures are shown in Fig. 3 for front excitation and in Fig. 4 for rear excitation.

DISCUSSION

Heat flow in a solid depends on the thermal conductivity λ, density ρ, and specific heat c. Such a flow is diffusive in nature; thus it is governed by a diffusion equation.

If the source periodicity is characterized by an angular frequency ω, in one dimension, the thermal-diffusion equation can be written as

$$\frac{d^2\Phi(x)}{dx^2}-\sigma^2\Phi(x)=-\frac{f(x)}{\lambda}\ , \tag{1}$$

where $\Phi(x)=\Theta(x)-\Theta$ is the difference between the sample temperature and PA-cell mean temperature, and $f(x)$ represents the heat source. Note that $\sigma^2=i\omega/\alpha$ depends on the thermal diffusivity of the material $\alpha=\lambda/(\rho c)$.

Figure 5 shows the excited-state manifold of the benzil crystal including the various proposed deexcitation processes (Jablonsky diagram). Absorption of the excitation light at 366 nm raises the molecular crystal to an excited singlet state of high energy $E(S_j)$.

It is well known[12] that, with a few exceptions such as azulene, the deactivation of the high-energy singlet state

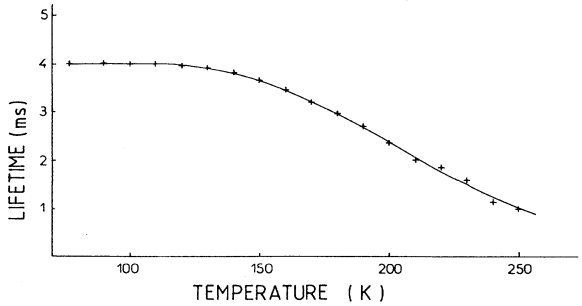

FIG. 2. Experimental phosphorescence lifetimes at different temperatures.

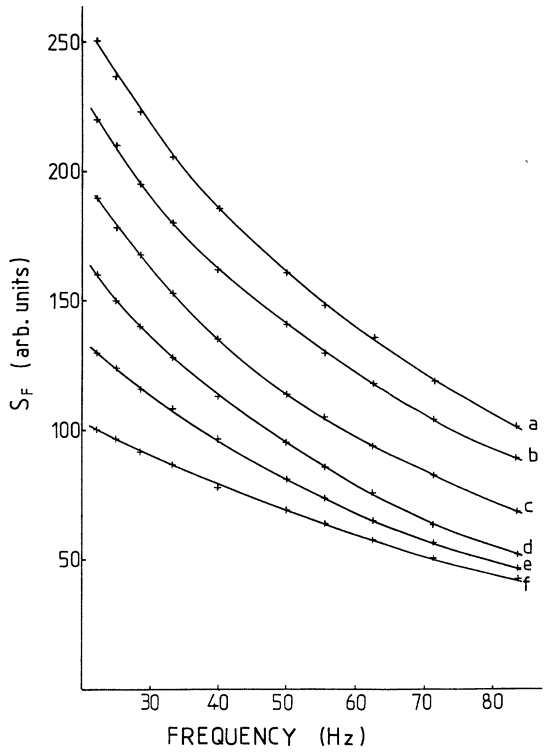

FIG. 3. Experimental plots of S_F vs f for a sample of thickness 200 μm at different temperatures: (a) $T=100$ K, (b) $T=120$ K, (c) $T=150$ K, (d) $T=170$ K, (e) $T=200$ K, (f) $T=240$ K.

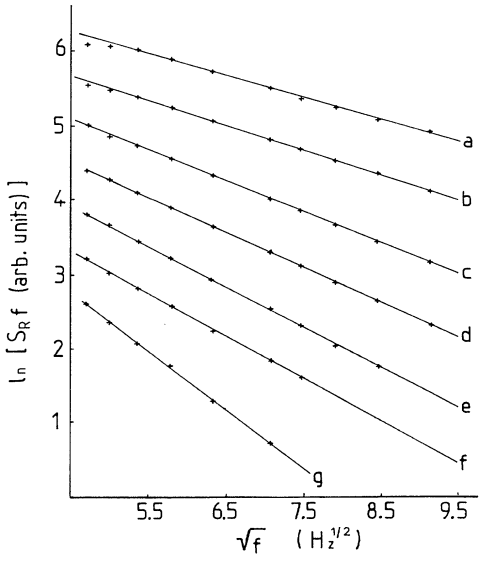

FIG. 4. Experimental plots of $\ln(S_R f)$ vs $f^{1/2}$ for a sample of thickness 100 μm at different temperatures: (a) $T=110$ K, (b) $T=130$ K, (c) $T=170$ K, (d) $T=200$ K, (e) $T=230$ K, (f) $T=250$ K, (g) $T=300$ K.

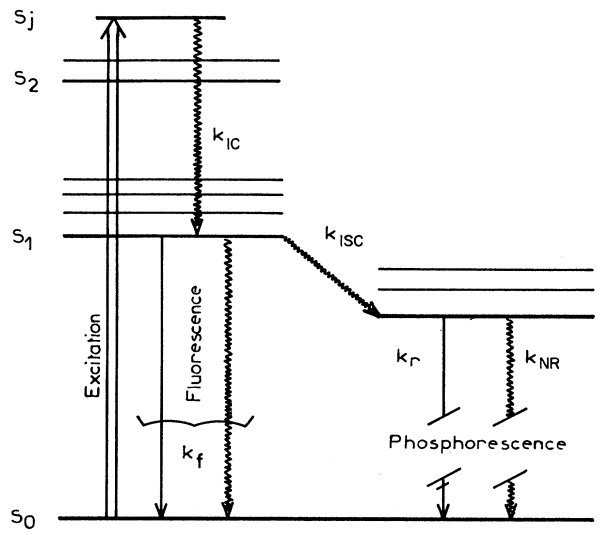

FIG. 5. Jablonsky diagram of benzil, radiative (→), and nonradiative (⇝) transitions.

S_j to the lowest-energy singlet state S_1 [with energy $E(S_1)$] involves a nonradiative internal conversion characterized by the probability-rate constant k_{IC} with an efficiency close to 100%.[12,13] In addition, in the case of aromatic ketones, the nonradiative singlet (S_1) to triplet (T) [with energy $E(T)$] intersystem crossing characterized by the probability-rate constant k_{ISC} is so efficient that the triplet-state quantum yield is in practice equal to unity.[13] So, we may consider that $k_{ISC} \gg k_f$, where k_f is the probability-rate constant of fluorescence, and that all the energy absorbed in the excited state S_j is transferred to the triplet state T. Then the heat source can be written as[14,15]

$$f(x)=k_{IC}n_j(x)\Delta E_s+k_{ISC}n_1(x)\Delta E_T+k_{NR}n_T(x)E(T) ,$$

where k_{NR} is the nonradiative probability rate constant of phosphorescence; ΔE_s is the energy difference between singlet states S_j and S_1; ΔE_T is the energy difference between the singlet state S_1 and the triplet state T; and n_j, n_1, and n_T are the populations of the excited state S_j, S_1, and T.

If $I=(I_0/2)[1+\exp(i\omega t)]$ is the incident monochromatic light flux and β denotes the solid optical absorption coefficient for the excitation length, the photon number at any point x (Fig. 6) due to light absorbed at this point in the sample is given by

$$\frac{\beta I \exp(-\beta x)}{E(S_j)} \quad \text{for the front excitation ,}$$

$$\frac{\beta I \exp[\beta(x-l_s)]}{E(S_j)} \quad \text{for the rear excitation .}$$

The populations of the excited states S_j, S_1, and T are obtained from the kinetic equations. For the front excitation, with k_{ISC} and $k_{IC} \gg k_f$, and k_{ISC} and $k_{IC} \gg \omega$, the resulting expressions are

$$n_j(x)=\frac{\beta I_0 \exp(-\beta x)}{2E(S_j)k_{IC}}, \quad n_1(x)=\frac{\beta I_0 \exp(-\beta x)}{2E(S_j)k_{ISC}} ,$$

$$n_T(x)=\frac{1}{k_r+k_{NR}}\frac{\beta I_0 \exp(-\beta x)}{2E(S_j)}\left[1+\frac{i\omega}{k_r+k_{NR}}\right]^{-1} .$$

Thereby, for the front surface excitation, the heat source can be written as follows:

$$f_F(x)=\frac{\beta I_0 \exp(-\beta x)}{2}\frac{\Delta E}{E(S_j)}\left[1+\frac{\eta_{NR}}{1+i\omega\tau}\frac{E(T)}{\Delta E}\right], \tag{2}$$

where $\tau=(k_r+k_{NR})^{-1}$ is the mean lifetime of the benzil-crystal phosphorescence, $\eta_{NR}=k_{NR}(k_r+k_{NR})^{-1}$ is the nonradiative quantum yield of benzil triplet state T and ΔE represents the energy difference between the excited states S_j and T.

With the same conditions, for the rear surface excitation, the heat source is given by

$$f_R(x)=\frac{\beta I_0 \exp[\beta(x-l_s)]}{2}\frac{\Delta E}{E(S_j)}\left[1+\frac{\eta_{NR}}{1+i\omega\tau}\frac{E(T)}{\Delta E}\right]. \tag{3}$$

In the thermal piston model[16] the PA signal is always generated by temperature variations at the gas-sample interface (Fig. 6).

The gas-sample interface temperature ϕ_0 can be written as[17]

$$\phi_0=-\frac{1}{\lambda_s}\int_0^{l_s} G(0,\xi)f(\xi)d\xi , \tag{4}$$

where $G(0,\xi)$ is the Green's function for both kinds of excitations.

The PA signal amplitude produced within the cell is given by[16]

$$S=\frac{\gamma P}{\sqrt{2}l_g\theta a_g}|\phi_0| , \tag{5}$$

where θ is the mean cell temperature a_g the inverse of the

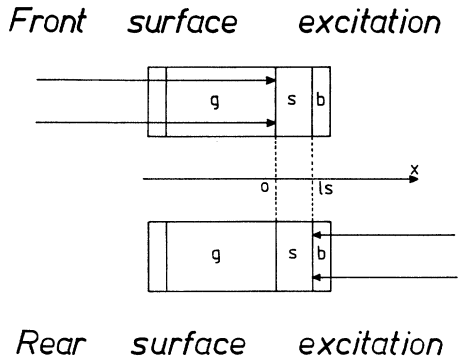

FIG. 6. Principle of the two excitations: b: backing, s: sample, g: gas.

gas thermal diffusion length, P the mean cell pressure, and γ the specific-heat ratio for the gas.

Our samples are optically opaque and thermally thick. Within these conditions, the detected PA signal amplitude may be written as follows (F stands for the front excitation and R for the rear one):

$$S_F = K_F \frac{1}{f} \left[\frac{(1+(1-\eta_r)[E(T)/\Delta E])^2+\omega^2\tau^2}{1+\omega^2\tau^2} \right]^{1/2} \frac{\Delta E}{E(S_j)}, \tag{6}$$

$$S_R = \frac{K_R}{f} \exp\left\{ -\left[\left[\frac{\pi l_s^2}{\alpha_s} \right]^{1/2} f^{1/2} \right] \right\} \times \left[\frac{\{1+(1-\eta_r)[E(T)/\Delta E]\}^2+\omega^2\tau^2}{1+\omega^2\tau^2} \right]^{1/2} \frac{\Delta E}{E(S_j)}, \tag{7}$$

where f is the incident beam modulation frequency, η_r the radiative quantum yield of benzil triplet state T, and K_F and K_R are given by

$$K_F = \frac{I_0}{2} \frac{\gamma P \alpha_g^{1/2} \alpha_s^{1/2}}{2\pi l_g \lambda_s \theta}$$

and

$$K_R = \frac{I_0}{b+1} \frac{\gamma P \alpha_g^{1/2} \alpha_s^{1/2}}{2\pi l_g \lambda_s \theta},$$

where b is the backing effusivity to sample effusivity ratio. In order to eliminate the influence of frequency-dependent coefficients and of temperature, we can define a term

$$\left[\frac{S_F(\theta_1)}{S_F(\theta_2)} \right]_f \left[\frac{S_F(\theta_1)}{S_F(\theta_2)} \right]_{f'}^{-1} \tag{8}$$

for two different temperatures θ_1, θ_2 and two different frequencies f and f'.

The phosphorescence intensity I_p is linearly dependent on radiative quantum yield η_r of triplet state as long as the extinction coefficient is temperature independent.[18] The values of radiative quantum yields $\eta_r(\theta_1)$ and $\eta_r(\theta_2)$, for temperatures θ_1 and θ_2, are related by

$$\eta_r(\theta_2) = \frac{I_p(\theta_2)}{I_p(\theta_1)} \eta_r(\theta_1) \tag{9}$$

Introducing (9) in (8), we obtain an equation in which only $\eta_r(\theta_1)$ is not deduced from experimental data.

$$\left[\frac{S_F(\theta_1)}{S_F(\theta_2)} \right]_f \left[\frac{S_F(\theta_1)}{S_F(\theta_2)} \right]_{f'}^{-1} = \left[\frac{\{1+[1-\eta_r(\theta_1)][E(T)/\Delta E]\}^2+\omega^2\tau_1^2}{(1+\{1-\eta_r(\theta_1)[I_p(\theta_2)/I_p(\theta_1)]\}[E(T)/\Delta E])^2+\omega^2\tau_2^2} \right]^{1/2} \left[\frac{1+\omega^2\tau_2^2}{1+\omega^2\tau_1^2} \right]^{1/2} \times \left[\frac{\{1+[1-\eta_r(\theta_1)][E(T)/\Delta E]\}^2+\omega'^2\tau_1^2}{(1+\{1-\eta_r(\theta_1)[I_p(\theta_2)/I_p(\theta_1)]\}[E(T)/\Delta E])^2+\omega'^2\tau_2^2} \right]^{-1/2} \left[\frac{1+\omega'^2\tau_2^2}{1+\omega'^2\tau_1^2} \right]^{-1/2}.$$

Solving this equation numerically for $\eta_r(\theta_1)$ by iterative method allows us to determinate the phosphorescence radiative quantum yield of benzil crystal. Such a method allows the determination of $\eta_r(\theta_1)$ as a function of temperature in the temperature range considered in this work, i.e., 100, 120, 150, 170, 200, and 240 K for the 200-μm-thick sample.

For a given temperature θ_1, we can choose five different values of temperature θ_2 and as many values of modulation frequencies f and f' as we want. For each value of θ_1 the determined value $\eta_r(\theta_1)$ corresponds to the average of the radiative quantum yield for five different values of θ_2 and for the modulation frequencies 22.2, 40, 60, and 83.3 Hz. From this method the accuracy in the determination of $\eta_r(\theta_1)$ is about 1%. The optical excitation energy $E(S_j)$ is 27 320 cm^{-1}. The lowest triplet-state energy $E(T)$ is 19 010 cm^{-1}. The variations of η_r for the benzil crystal as a function of temperature are shown in Fig. 7.

Using an approximation method introduced by Rockley and Waugh[19] and extended by Mandelis,[20] we have estimated in a previous work[21] the radiative quantum yield of benzil triplet state. Results are plotted in Fig. 7. We can note that this approximation deviates about 10% at low temperatures where triplet-state mean lifetime τ reaches its maximum.

Given that we have determinated benzil triplet-state quantum yield η_r and that we have deduced the excited-state energies, the triplet-state lifetime, and the thickness

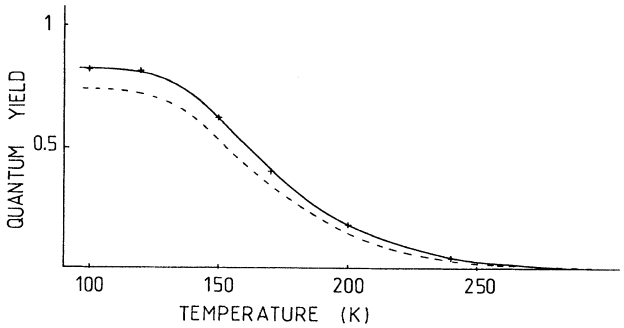

FIG. 7. Variation of the radiative phosphorescence quantum yield of benzil with temperature: ——: present work; — — —: Rockley and Waugh method.

of the sample from experimental data, the PA signal fitting depends only on thermal diffusivity α_s of the sample. The fitting of calculated values of $\ln(S_R f)$, from Eq. (7), to the experimental values allows the determination of α_s within 2% precision. The results of the fitting are shown in Fig. 4. The variations of benzil thermal diffusivity as a function of temperature are shown in Fig. 8. The values of α_s justify *a posteriori* the choice for the thickness of the sample. In fact, it is well known that the sample on rear excitation can be considered as thermally thick when $a_s l_s \geq 1.6$.[17,22]

It is interesting to evaluate the influence of η_r and τ [see Eq. (7)] in the determination of α_s. If we neglect η_r and τ, Eq. (7) reduces to

$$S_R = \frac{K_R}{f} \exp\left\{ -\left[\left(\frac{\pi l_s^2}{\alpha_s} \right)^{1/2} f^{1/2} \right] \right\} .$$

The thermal diffusivity may be deduced from the slopes p of $\ln(S_R f)$ versus $f^{1/2}$.

Experimentally, for benzil crystals, the curves $\ln(S_R f)$ as a function of $f^{1/2}$ are nearly straight lines. We have calculated $\alpha_p = \pi l_s^2 / p^2$ from the curves in Fig. 4. The variations of α_p as a function of temperature are shown in Fig. 8.

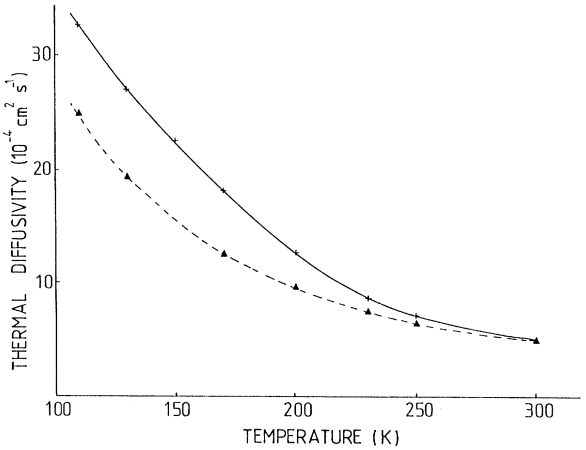

FIG. 8. Experimental dependence of α on temperature for benzil crystals: (+) denote α_s; (▲) denote α_p.

The 30% difference between α_p and α_s for temperatures near 180 K shows the importance for benzil crystals of η_r and τ in the determination of α_s.

[1] *Photoacoustic and Thermal Wave Phenomena in Semiconductors,* edited by A. Mandelis (North-Holland, New York, 1987). *Physical Acoustics, Principles and Methods,* edited by W. P. Mason and R. N. Thurston (Academic, Boston, 1988), Vol. 18.

[2] E. Kanezaki, Mol. Cryst. Liq. Cryst. **166**, 245 (1989).

[3] K. Razi-Naqvi, M. S. Adili, and M. E. Abu-Zeid, Chem. Phys. Lett. **111**, 279 (1984).

[4] V. Upadhyaya, L. B. Tiwari, and S. P. Mishra, Spectrochim. Acta, Part A **41**, 833 (1985).

[5] J. E. Sabol and M. G. Rockley, J. Photochem. Photobiol. A Chem. **40**, 245 (1987).

[6] P. Charpentier, F. Lepoutre, and L. Bertrand, J. Appl. Phys. **53**, 608 (1982).

[7] P. Korpiun, R. Tilgner, and D. Schmidt, J. Phys. (Paris) Colloq. **44**, C6-43 (1983).

[8] A. Torres-Filho, L. F. Perondi, and L. C. M. Miranda, J. Appl. Polym. Sci. **35**, 103 (1988).

[9] T. Hashimoto, J. Cao, and A. Takaku, Thermochim. Acta **120**, 191 (1987).

[10] S. C. Bera, R. Mukherjee, and M. Chowdhury, J. Chem. Phys. **51**, 754 (1969).

[11] I. Y. Chang and B. N. Nelson, J. Chem. Phys. **62**, 4080 (1975).

[12] S. P. McGlynn, T. Azumi, and M. Kinoshita, *Molecular Spectroscopy of the Triplet State* (Prentice-Hall, Englewood Cliffs, NJ, 1969).

[13] F. Wilkinson, in *Organic Molecular Photophyiscs,* edited by J. B. Birks (Wiley, London, 1975), p. 145.

[14] R. S. Quimby and W. M. Yen, J. Appl. Phys. **51**, 1780 (1980).

[15] A. Mandelis, Y. C. Teng, and B. S. H. Royce, J. Appl. Phys. **50**, 7138 (1979).

[16] A. Rosencwaig and A. Gersho, J. Appl. Phys. **47**, 64 (1976).

[17] B. Bonno, J. L. Laporte, and Y. Rousset, J. Appl. Phys. **67**, 2253 (1990).

[18] *Introductory Survey of Molecular Spectra in Chemical Applications of Spectroscopy,* edited by W. West (Wiley Interscience, New York, 1968), Part 1, p. 46.

[19] M. G. Rockley and K. M. Waugh, Chem. Phys. Lett. **54**, 597 (1978).

[20] A. Mandelis, Chem. Phys. Lett. **91**, 501 (1982).

[21] J. L. Laporte, B. Bonno, and Y. Rousset, J. Photochem. Photobiol. **45**, 215 (1988).

[22] M. J. Adams and G. F. Kirkbright, Analyst (London) **102**, 281 (1977).